Ferrites for chokes in commutation motors

The high current required by DC commutation motors necessitates a careful selection of ferrites for EMI suppression.

MARTA SAN ROMAN
Philips Components
Guadalajara, Spain

Electric motors have a more extensive presence in our lives than we realize. They can be found in such diverse areas as entertainment (CD players, cameras, video recorders), personal computers (fan motors, disk drives), and everyday living (watches, sewing machines, fans, razors, air-conditioners, food processors, dishwashers).

In general, there are three large categories of motors: AC motors, driven by the commercial network (50 or 60 Hz), are used, for example, in refrigerators, dishwashers, vacuum cleaners, coffee mills, ventilators and Rototillers. DC motors, which take energy from a battery, are used in hair dryers, electric razors and cars. Precision motors, like brushless DC motors and stepping motors, are used for speed and positioning control.

Including our home and our cars, and the three kinds of motors, an average family will have more than 100 motors. This is an indication of how much they are used and what a big problem they would cause if the interference is not controlled. This article will focus on the DC commutation motors used in cars.

In the automotive industry, first FM radio reception (86–108 MHz), and later electronic control and management were introduced, and thus EMI suppression became a critical issue. The number of motors in a car is still increasing (Figure 1). DC commutator motors, like starter motors, windshield wiper motors, radiator-cooling fans, fuel pumps, electric windows, door locking, mirror positioning or sunroof operators, among others, can cause interference. The most important characteristic of these motors is the high current they need, which is up to a few tens of amperes.

Due to the high currents, ferrite beads and wideband chokes would certainly saturate. Current-compensated or iron powder cores require expensive winding operations. A good solution is a ferrite rod with a solenoid winding directly on the core. The open circuit of the rod has a low effective permeability with high current carrying capability, while the lower inductance is not a problem since the frequency is FM band.

It is very important that these chokes (rod + coil) areas are as close to the brushes as possible. Since it is very high frequency noise, emissions can easily change from conducted to radiated.

To create great impedance, the rod is wound over the full length. The maximum number of turns follows from the minimum wire diameter, corresponding to the current rating.

The ferrite material, therefore, must have a high Curie temperature, Tc, (mo-

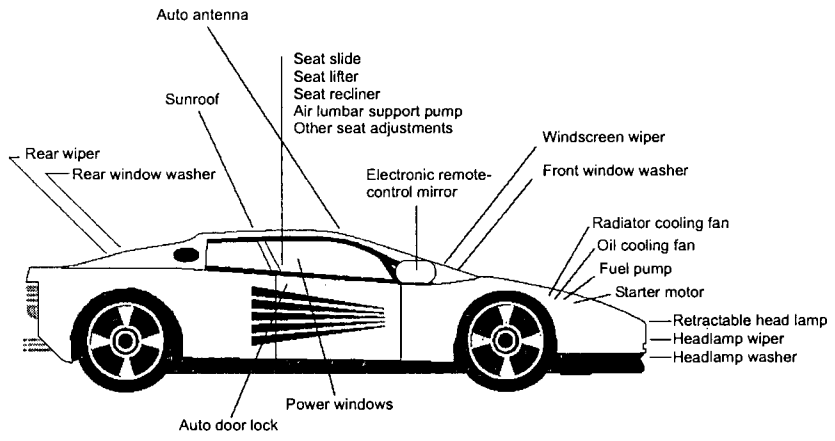

Figure 1. Small motors in a car.

tor temperature will exceed 100° C) and high saturation, Bsat. A high resistivity, ρ, is indispensable as well, to avoid short-circuits when the winding sits directly on a non-coated core. The importance of these three parameters (Tc, Bsat and ρ) makes nickel-zinc (NiZn) or manganese-zinc (MnZn) with increased resistivity (10^4 Ω m!) grades especially suitable for these automotive applications and, as a natural extension, also suitable for suppressing EMI in electric power tools.

An extra advantage of MnZn ferrite rods is that they have a higher mechanical strength, which considerably reduces the risk of breakage of the core when the coil is wound or during automatic insertion.

TEST AND MEASUREMENT

The relevant parameters for EMI suppression differ completely from the ones in an antenna rod application. Inductance and Q-factor are not of interest, but impedance, Z, or attenuation/insertion loss, IL, at the EMI frequencies are. Therefore, measurements are carried out in an impedance analyzer (Z) or in a network analyzer (IL). If the test requires the application of a high bias current, a power supply is needed, along with a special LC filter with 2 functions:

- Protecting the measurement equipment from the DC current.
- Eliminating the influence of the power supply on HF measurement.

A typical filter used for this kind of test could be constructed according to VDE 0565 (Part 2/9.78) and DIN 57 565 (Part 2).

At RF frequencies, a ferrite choke shows high impedance which suppresses unwanted interference. The resulting voltage over the load impedance will be lower than without the suppression component. The ratio of the two is the insertion loss (Figure 2).

The insertion loss is expressed logarithmically:

$$IL = 20 \log_{10}(E_0/E) \text{ dB}$$

$$IL = 20 \log_{10} \frac{|Z_G + Z_L + Z_S|}{|Z_G + Z_L|} \text{ dB}$$

where

E = load voltage with inductor

E_o = load voltage without inductor

For a 50-ohm/50-ohm system:

$$IL = 20 \log_{10}(1 + Z/100) \text{ dB}$$

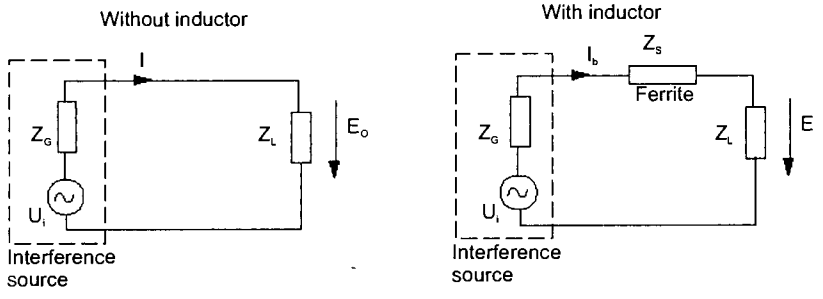

Figure 2. Equivalent circuit.

To express insertion loss in dB seems very practical because interference levels are usually expressed in decibels as well. But beware! Insertion loss depends on source and load impedance, so it's not a pure product parameter like impedance. In final applications, source and load are seldom 50-ohm fixed resistors. They might be reactive, frequency dependant and quite different from 50 ohms. To reiterate, insertion loss is a standardized parameter for comparison, but it won't directly predict the attenuation in the actual application.

EXAMPLE OF INSERTION LOSS

Rod 6.5 - 0.3 x 25 ± 0.6

Ferrite material: MnZn with increased resistivity (ρ = 10^4 Ω m)

14 turns of wire Cu ϕ = 1.6 mm

I_{DC} = 26 A

The insertion loss would be as shown in Figure 3.

SATURATION AND TEMPERATURE

Choke design (ferrite rod and coil) and DC should be such that for the rated DC current, the two major negative effects on its attenuation are kept within limits. These effects are:

- Saturation
- Heating

The cross-section (effective area) of the ferrite core is inversely proportional to saturation and directly proportional to attenuation. And the larger the rod, the longer it takes to heat it.

0 A		26 A	
Conditions	IL	Conditions	IL
50 MHz, 25° C	≈ 20 dB	50 MHz, 140° C	≈ 18 dB
100 MHz, 25° C	≈ 28 dB	100 MHz, 140° C	≥ 22.5 dB
200 MHz, 25° C	≈ 29 dB	200 MHz, 140° C	≈ 30 dB

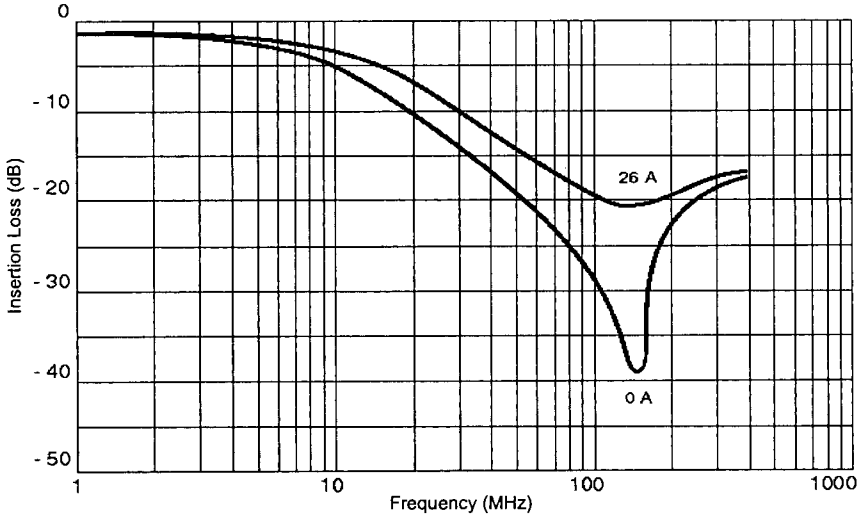

Figure 3. Insertion loss with and without DC bias.

If the coil consists of thin wire and many turns, *saturation* limits the performance. In this case, current is not very large and heating is not the real problem. Once the bias is on, the change in Z or IL characteristics with respect to the non-magnetized state (0 A) remains stable. This means that it does not matter how long the current is applied, since temperature rise will be small and does not affect the behavior of the choke.

In the case of thick wire and fewer turns, *temperature* is the limitation; now DC currents are higher and dissipation due to the resistance of the copper winding will heat up the ferrite. This will decrease the saturation level and the impedance characteristics of the material. Z and IL curves will start changing until an equilibrium temperature is reached.

These factors have to be taken into account when designing a choke. The application itself will determine the final performance, because the DC current is not applied for a long time in every case. For example, the motors of an electric window or sunroof are only working for a few seconds, so there is no time for a serious temperature rise. But fuel pumps or some ventilators are continuously on, so temperatures can become very high and stabilize at these levels.

Table 2 shows two choke designs. Design 1 has lower bias, so saturation is much smaller. This is due to both the lower DC current and the fact that lower operating temperature is achieved. The second design supports larger I_{DC} and therefore temperature rise is higher, so it becomes more saturated and the difference with and without biasing is also more noticeable.

Figures 4 and 5 show the influence of different current levels on the insertion loss from 25° C to the operating (specified) temperature. For Design 1, the "softer" conditions result in the choke not changing too much from 0 A to the maximum 7 A; temperature only reaches 40° C and the rod does not get saturated (the IL curve does not change much). For Design 2, the situation is different; the different steps between 0 A at 25° C to 26 A at 140° C show a larger variation in temperature and saturation (a big shift in the IL curve).

Figures 6 and 7 (for Design 1 and 2, respectively) show the influence of temperature under maximum bias. IL is measured three times: without bias, immediately after bias and with the bias being applied for enough time to reach the equilibrium temperature (the point from which IL does not decrease further). Again, for Design 1 the change is much smaller than for Design 2.

CHOKE DESIGN

The function of these chokes is to suppress EMI at certain frequencies in DC commutator motors. The most common interval is 50 to 200 MHz. For this purpose, it is necessary to achieve the maximum impedance or attenuation within that range.

The best solution is a rod wound with a single layer over the full length. Additionally, a large DC current causes an increase of temperature and/or a high premagnetization of the rod.

SELECTING THE CHOKE

From the application point of view, the thicker the rod, the better it would be: the more cross section (effective area), the less saturation

	Design 1	Design 2
Rod dimensions	3 x 17	6.5 x 25
Ferrite material	MnZn with increased resistivity (ρ = 10^4 Ω m)	MnZn with increased resistivity (ρ = 10^4 Ω m)
Coil	17 turns of Ø0.85 mm wire	14 turns of Ø1.6 mm wire
DC current	7 A	26 A

Table 2. Choke designs compared.

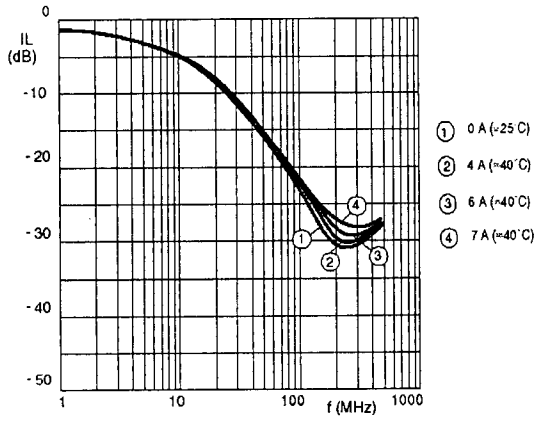

Figure 4. Design 1: IL versus frequency at different I_{DC}.

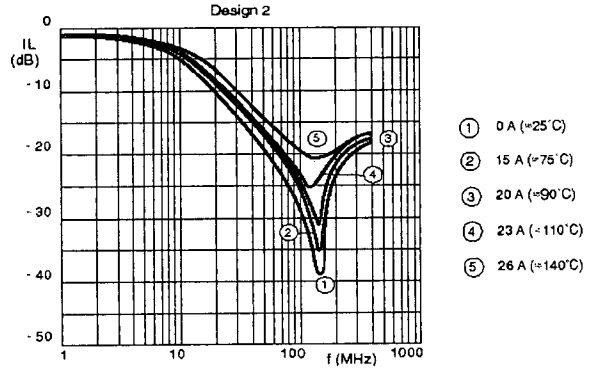

Figure 5. Design 2: IL versus frequency at different I_{DC}.

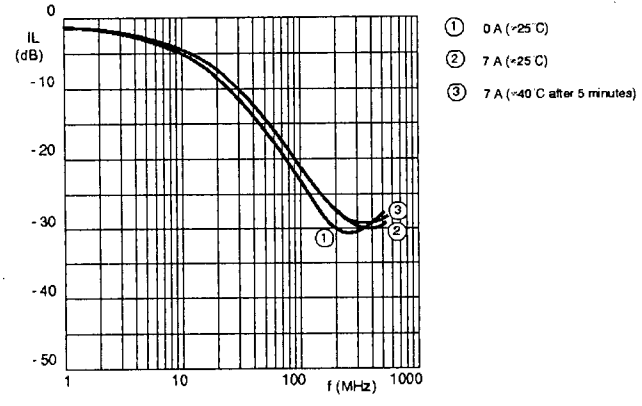

Figure 6. Design 1: Influence of temperature on IL under maximum bias.

and the more attenuation, and moreover, the larger current it can withstand without heating. But some other considerations, such as a limited space or low cost, make the rod and coil selection a critical issue.

Impedance and attenuation depend on the mechanical dimensions of the rod, but hardly on the material permeability at the lower frequencies. Other material parameters, like Curie temperature, resistivity and saturation, are of importance.

At the higher frequencies, the winding plays the main role; the performance is limited by the parallel capacitance of the winding and not by the ferrite properties.

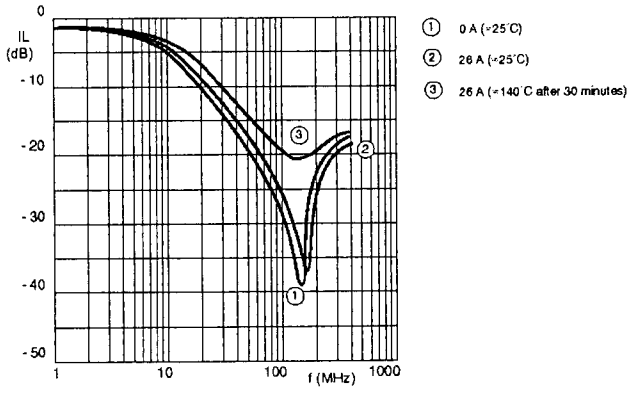

Figure 7. Design 2: Influence of temperature on IL under maximum bias.

The DC current is specified by the application. From the data of current and the duration of its application, a suitable wire type should be chosen: enameled, wire thickness depending on the current density, resistance per unit length, and so on.

The maximum number of turns follows from the rod length and wire diameter. Impedance (or attenuation) level is proportional to the square of the number of turns.

CONCLUSION

The performance of a suppression choke under bias conditions is defined by a combination of all the following parameters:

- Rod size
- Material characteristics
- Wire diameter
- Number of turns
- DC current
- Duration of current
- Operating conditions (temperature)

The main effects of DC current on the choke are saturation and heating. Performance of the choke may change because of these effects.

BIBLIOGRAPHY

Philips Magnetic Products. Technical note, "3S3, A New Soft Ferrite for EMI-suppression."

Tak Kenjo: "Electric Motors and their Controls," Oxford Science Publications, 1991.

Ramshaw and van Heeswijk: "Energy Conversion Electric Motors and Generators," Saunders College Publishing, HRW, 1990.

MARTA SAN ROMAN *studied physics at the University of Salamanca, Spain, and specialized in electronic physics. After receiving her degree in 1990, she joined the Magnetic Products Division of Philips Components as a development engineer at Hispafer, a ferrite manufacturing facility located in Guadalajara. There she was mainly involved with ferrite materials, process improvement, core designs, and measuring methods. In 1994 she became the application engineer for the range of ferrites for EMI suppression. marta.sanroman@es.ccmail.philips.com.*

sign value. Miniature metallized polyester film, 100 VDC capacitors are recommended because of their small size and low cost.

The 62.3-mH center-tapped inductors for L1 and L4 can be realized with two surplus 88-mH toroidal inductors originally used as telephone-line loading coils by the telephone company. Applications using these surplus inductors were discussed in an article published in an amateur radio magazine.[7] These inductors are available from the author for those wishing to build this filter. Send a SASE to the author for details and include an explanation of your application. If you want a copy of the article mentioned, include $3.00.

Although the surplus inductors are 88 mH, they are unpotted and wound with bifilar wire so they can be easily modified to a smaller inductance by removing turn pairs until the desired inductance is reached. The bifilar windings are connected in series aiding by connecting the red start lead to the green finish lead. This junction also serves as the center taps for L1 and L4.

Referring again to Figure 3, L2 and L3 are noted as being 12.3 mH and 485.2 mH. The ratio of these two values is about 39, and although this ratio is larger than preferable, it is still within reason. As the ratio of the largest component relative to the smallest component increases beyond 100, there will be a question regarding whether or not the design is practical and some design changes may be necessary to reduce the ratio.

The value of L3 is 485 mH, and six surplus 88-mH inductors would normally be required to realize just L3. When including L1, L4 and L2, the total number of inductors will be nine. To reduce the number of surplus inductors needed to build this filter, the series branch comprised of resonators 2 and 3 was moved to connect between the center taps of L1 and L4. By making this change, the C2 and C3 values increased by four times and the L2 and L3 values decreased to one-quarter of their original values. L3 now becomes 485.21/4 = 121.3 mH and L2 becomes 12.349/4 = 3.09 mH. L3 can now be realized with only two 88-mH inductors, one inductor being modified so when connected in series with the other, the sum of their individual inductances is within 1 percent of 121 mH.

The L2 value of 3.09 mH is realized by removing all the windings from an 88-mH inductor and then winding the bare core with 71 turns of #24 bifilar magnet wire 82" long with the two windings connected in series aiding. The moly perm core used in the surplus 88-mH inductors has an OD, ID and HT of .928, .567 and .350 inches, respectively, and is equivalent to Magnetics Part No. 55347 with a permeability of 200.

Capacitors C2 and C3 of 0.145 mF and 5.70 mF were realized with metallized polyester film capacitors. C2 consists of two capacitors in parallel selected to be within 1 percent of the design value. C3 is a parallel combination of 4.7-mF and 1.0-mF capacitors also selected to be within 1 percent of the design value. The realization of the BPF was satisfactorily completed using these inductors and capacitors.

Figure 5 is a photo of the assembled Cauer BPF using the components previously described. The components are widely spaced on a piece of cardboard to clearly show the assembly details. However, if the BPF is to be used in the lab, each toroidal inductor can be put on edge and stacked side-by-side to make a more compact assembly suitable for installation in a small aluminum box. Because a toroidal winding has the property of containing its magnetic field within the core, there is essentially no external coupling between the inductors. Consequently, the inductors can be stacked together with cardboard spacers used to separate the windings. The inductors and capacitors are conveniently secured to the cardboard base with silicone sealer.

Before the surplus toroidal inductors were considered as a means of realizing this particular design, the question of whether the inductors have sufficient Q had to be answered. Knowing the BPF 3-dB pass-

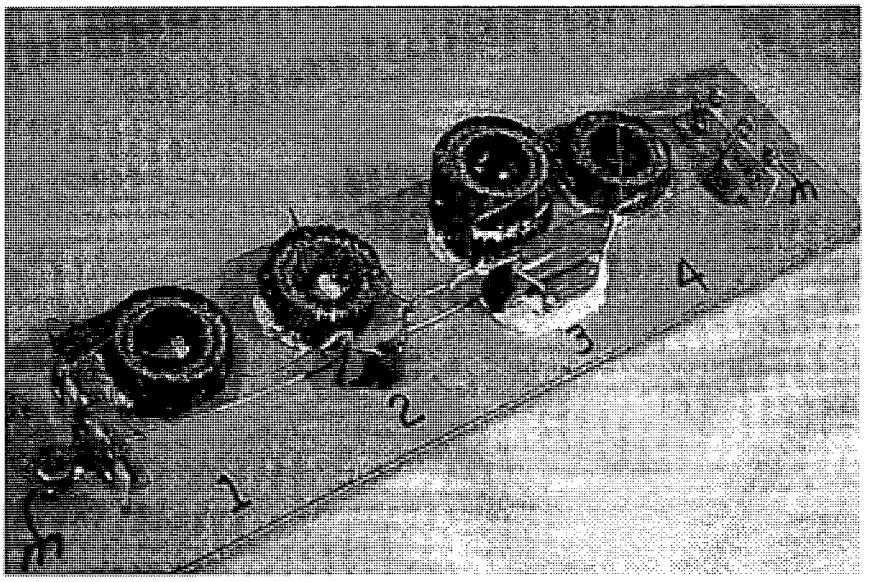

Figure 5. The assembled Cauer BPF with the components described in the text mounted on a 2-1/4 X 8-1/2-inch piece of cardboard. Resonators #2 and #3 are connected together and between the L1 and L4 center-taps so the C2, C3, L2 and L3 values are convenient to realize. In the assembled BPF, C2 and C3 are 0.145 µF and 5.70 µF, while L2 and L3 are 3.09 mH and 121 mH, respectively. Figure 6 shows the measured responses.

band and the center frequency, the inductor minimum Q required by the design can be estimated with the equation: $Q_{min} = 20\ F_c/B3$, where F_c is the BPF center frequency and B3 is the 3-dB bandwidth, both in kHz. Using this equation, $Q_{min} = 20 \bullet 1.2/3.3 = 7.27$. If the inductor Qs are all greater than 7.3 at all frequencies associated with this design, then the measured attenuation response should be virtually identical with the theoretical response.

From previous measurements made on these surplus inductors,[8] the Q of L1 and L4 at 1.2 kHz is estimated to be greater than 50. The Q of L2 (3.09 mH) at 7.52 kHz was measured to be 64, and at 1.2 kHz was estimated to be about 10. The Q of L3 (121 mH) at 191 Hz was measured to be 12, and at 1.2 kHz was estimated to be 75. Because all inductor Qs are greater than the minimum required Q of 7.3, the measured attenuation response of the assembled BPF should be virtually identical with the computer-calculated response shown in Figure 4.

MEASUREMENT OF BPF ATTENUATION AND RETURN LOSS

Although the inductor's Qs are satisfactory for this application, the effect of one variable cannot be anticipated by the computer simulation; the change of BPF attenuation and return loss that might occur after resonators 2 and 3 are moved from the tops of L1 and L4 and reconnected at the center taps. Consequently, it is necessary to measure both the attenuation and return loss responses of the Cauer BPF to be assured that the computer-calculated responses shown in Figure 4 are actually realized.

RELATIVE ATTENUATION

Because the 48-ohm source and load terminations of the BPF (Figure 3) are within 4 percent of 50 ohms, it is possible to use a standard 50-ohm test system to test the BPF without introducing any discernible error. A 50-ohm signal generator (SG) was connected to a 50-ohm load with a wideband, high-impedance AC milli-voltmeter connected across the load. The ac milli-voltmeter must have a 1-dB bandwidth greater than 20 kHz. The SG frequency was set to 1.2 kHz and adjusted for a near maximum output level. The BPF was then inserted between the SG and the load. A decrease in the load voltage of less than 0.2 dB was noted and was recorded as the insertion loss of the BPF. With the BPF still in the test circuit, the SG voltage was increased by 0.2 dB and the output meter level was recorded as the 0-dB reference level. The SG frequency was then varied from 1.2 kHz to 50 Hz and then to 20 kHz, while the corresponding load voltage levels were recorded in dB relative to the 0 dB level at 1.2 kHz. The resulting measured relative attenuation response is shown in Figure 6.

Except for the F3 attenuation peak, all other frequency/attenuation points on the measured attenuation response curve closely agree with the computer-calculated response shown in Figure 4. The reason the measured attenuation at frequencies between 150 and 200 Hz are slightly in error is attributed to SG harmonics falling in the 500-3000 Hz passband of the BPF and being passed unattenuated to the load and output voltage indicator. The presence of these SG harmonics gives an incorrect indication of the BPF having less attenuation between 150 and 200 Hz than it actually has. This effect of SG harmonic distortion may be minimized or eliminated by using a SG having lower harmonic distortion or by using a tuned detector such as a network analyzer or a spectrum analyzer.

Of particular interest in the attenuation response is that after the attenuation peaks are reached, the attenuation drops to a minimum of 30 dB below 191 Hz and above 7.52 kHz. This is the minimum level of stopband attenuation (A_s) that was specified for this Cauer design, and the measured attenuation response shows that this specification was achieved. Also, note that the attenuation peak at 7.52 kHz is relatively sharp and rises about 15 dB above the 30-dB A_s level. The sharpness of the peak indicates that the L2 inductor (3.09 mH) has more than adequate Q at resonance. If the L2 Q was very low, the attenuation peak at F2 could be rounded with perhaps only a slight rise over the 30-dB level. The same may be said for

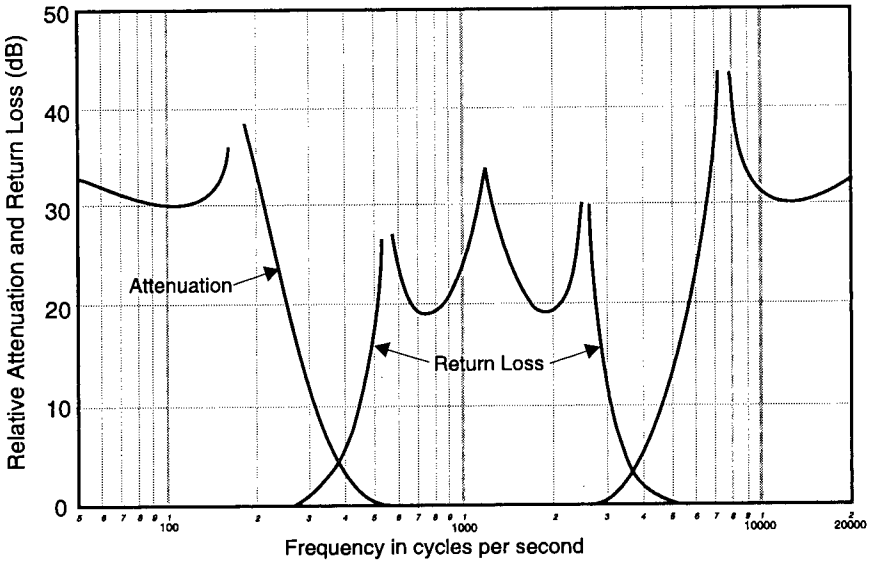

Figure 6. The measured relative attenuation and return loss responses of the assembled Cauer BPF shown in Figure 5. The attenuation response was measured relative to the 0 dB reference at 1.20 kHz. The insertion loss at 1.20 kHz was less than 0.2 dB.

the attenuation peak at F3 (191 Hz), except that the peak at F3 would be higher if the SG harmonics in the BPF passband were absent.

Whenever a Cauer BPF is tested for attenuation, these distinctive characteristics should be noted, and in particular, problems should be anticipated that relate to the ability to accurately measure the stopband attenuation at those lower frequencies where the signal generator harmonics fall in the BPF passband

RETURN LOSS

Although the attenuation test results of the Cauer BPF gives a good indication that the BPF was correctly designed and assembled, this test by itself is not conclusive proof that everything is in order. In addition to the attenuation test, the BPF should be tested for return loss (RL). The RL test is more appropriate for testing the BPF passband response as it is more sensitive to errors in design or assembly over this portion of the BPF response than is the attenuation test. In short, the attenuation test is used primarily for checking the BPF stopband for attenuation levels greater than 3 dB, and the RL test is used for checking the BPF passband for RL levels greater than 3 dB.

The Cauer BPF was tested for RL using the 50-ohm low-frequency return loss bridge (RLB) described in Reference 9. Although a 50-ohm plug-in resistor network was used with the RLB, and the Cauer BPF is designed for 48-ohm terminations, the difference in impedance levels is small enough that the test results were not affected. Figure 6 shows the measured RL response, and it is in good agreement with the computer-calculated RL response shown in Figure 4. The measured RL minimum is slightly less than the design RL minimum of 20.5 dB, but this is typical of the difference that is to be expected between the design and measured RL values. The main thing to note in the measured RL response is the presence of three peaks (for the 3rd-order Cauer BPF), with the center peak being at the BPF center frequency of 1.2 kHz, and the sides of the RL response dropping to near 0 outside the BPF passband. The fact that the two troughs of the RL response are at the same level (about 19.5 dB) as shown in Figure 6 indicates that resonators 2 and 3 are correctly tuned. If the tuning was incorrect, the two troughs would be at different levels or completely absent.

The fact that the attenuation and return loss plots increase in a downwards direction in Figure 4 and upwards in Figure 6 should cause no confusion. The ELSIE software is programmed to plot increasing loss downwards, whereas plotting increasing loss upwards is preferred. Consequently, the computer-plotted responses increase in a downwards direction while the hand-plotted responses increase upwards.

SUMMARY

For those bandpass filtering applications requiring better selectivity than available with a 3rd-order Chebyshev response, a 3rd-order Cauer BPF was suggested as a more selective replacement. After comparing the advantages and disadvantages of these two filter types, the main disadvantage of the Cauer (its difficulty of design) was solved by using free filter design and analysis software available from Trinity Software.[6] Using the free ELSIE software, it was demonstrated that a 3rd-order Cauer BPF with a 30-dB stopband specification could be designed having a passband specification identical to that of the 3rd-order Chebyshev BPF. The Cauer BPF was realized using surplus high-Q toroidal inductors available from the author and standard commercial capacitors.

Measurement of the Cauer BPF attenuation and return loss confirmed that the expected performance was achieved and the Cauer BPF was more selective than the Chebyshev, having about 2/3 of the 30-dB bandwidth of the Chebyshev. The article clearly demonstrates that the design and assembly of any 3rd-order Cauer BPF is within the capability of the average EMI technician or engineer.

This concludes comments regarding the attenuation and RL measurements of the 3rd-order Cauer BPF designed to replace the less selective Chebyshev BPF. The measured response curves demonstrate that the Cauer BPF design has a 30-dB bandwidth that is about 2/3 that of the Chebyshev BPF and the Cauer BPF is practical because of the close agreement between the computer-calculated and measured responses of attenuation and return loss. Those readers attempting to duplicate this Cauer BPF design or other similar designs should have similar success.

The procedure demonstrated in the design of an audio bandpass filter is equally applicable to the design of RF BPFs. All engineers and technicians having a genuine test application for the high-quality toroidal inductors described in this article are encouraged to write to the author for instructions on how to obtain a limited quantity of the inductors for their personal use and experimentation.

REFERENCES

1. E. Wetherhold, "Audio Filters for EN55020 Testing," *ITEM 1998*, p. 36.
2. Philip J. Davis, *The Thread, A Mathematical Yarn*, 2nd edition, (New York, Harcourt Brace Jovanovich, Publishers, 1989). A series of delightful yarns about mathematics and mathematicians with the spelling of Chebyshev's name used as the historical "thread" to join the various yarns.
3. *A Handbook on Electrical Filters*, Table 4.4, Element Values of Chebyshev Lowpass Filter Prototypes, (Rockville, Maryland, White Electromagnetics, Inc., 1963) p. 101.
4. Arthur B. Williams and Fred J. Taylor, *Electronic Filter Design Handbook*, 2nd edition, Tables 11-27 through 11-31, (New York, McGraw-Hill Publishing Co. 1988.) pp. 11-24 to 11-36.
5. *The 1998 ARRL Handbook for Radio Amateurs*, 75th Edition, Table 16.2, Element values of Chebyshev lowpass filters, (Newington, CT, The American Radio Relay League, 1997) p. 16.12.
6. ELSIE Filter Design and Analysis Program

continued on page 253